VIP *Very Important Paper*

Gelation Kinetics-Structure Analysis of pH-triggered Low Molecular Weight Hydrogelators

Vasudevan Lakshminarayanan,[a] Cindhuja Chockalingam,[a] Eduardo Mendes,[a] and Jan H. van Esch*[a]

Properties such as shear modulus, gelation time, structure of supramolecular hydrogels are strongly dependent on self-assembly, gelation triggering mechanism and processes used to form the gel. In our work we extend reported rheology analysis methodologies to pH-triggered supramolecular gels to understand structural insight using a model system based on N–N′ Dibenzoyl-L-Cystine pH-triggered hydrogelator and Glucono-δ-Lactone as the trigger. We observed that Avrami growth model when applied to time-sweep rheological data of gels formed at lower trigger concentrations provide estimates of fractal dimension which agree well compared with visualization of the microstructure as seen via Confocal Laser Scanning Microscopy, for a range of gelator concentrations.

1. Introduction

Supramolecular gels formed by the self-assembly of low molecular weight hydrogelators (LMWGs) are an important class of supramolecular materials. With applications ranging from cell culture scaffolds, drug delivery systems, they are emerging as an alternative to their polymer counterparts.[1,2] A number of triggering methods exist to initiate the self-assembly of LMWGs namely temperature, pH, light, sound, chemical fuels, enzymes etc.[2–7] Each of these triggering methods enable to achieve a certain of degree of control and opens up the possibilities to create a different applications of supramolecular gels using them. In the context of applications, in order to optimize formulations, it is imperative that the triggering method and processing of LMWGs be related to the material properties that are obtained in gels. Thus, creating a link between gel processing and resulting characteristics is important. Controlled gel processing by temperature programming, solvent switch and addition of additives have been demonstrated to impact structure and properties of organogels.[8–10] Later reports have suggested and encouraged the notion that such ideas may be valid for hydrogels as well. Control over gelation conditions using Glucono- δ -Lactone (GDL) paved the way to a number of studies investigating the effect of kinetics on mechanical properties of Fmoc-dipeptide hydrogels.[11,12] Depending on the variant of the gelator chosen, different properties in terms of shear modulus were obtained for the same triggering method. Due to the impact of processing conditions on gel properties, it is important to include gel triggering method in structure-property investigation. Temperature-triggered organogelators have been well studied in this regard and clear structure-property relationships have been developed.[8–10] However, it is not the case for hydrogelators. In the recent years, considerable attention has been given to pH-triggered supramolecular hydrogels obtained from eg. dipeptide hydrogelators, sophorolipids due to their versatility.[3,4,28] In this work we investigate the effect of kinetics of pH triggering on the obtained gel properties and microstructure. Already developed structure-property relationships from temperature triggering of organogelators were used to understand if such an approach can be valid for hydrogelators as well. For the sake of simplicity, we used an off-the-shelf dipeptide gelator (Dibenozyl-L-Cystine (DBC)) as an acid-triggered hydrogelator, in combination with GDL.[11,13,14]

2. Results and Discussion

First, the pH triggering system by GDL hydrolysis was studied to ensure that it could serve as a reliable method for the kinetic studies of gelation. The kinetics of pH change of a 5 mM solution of Na_2DBC observed after addition various amounts of GDL is shown in Figure 1. Upon addition of GDL, pH decreases rapidly within the first minute followed by a more gradual change over the course of tens to hundreds of minutes. After a certain time (ca. 100 min), the pH does not change significantly. Increasing the amount of GDL added resulted in a faster decrease in pH and a lower final pH value (measured after 8 hours) (Figure 1A). We observed that changing the gelator concentration had a minor effect on the observed final pH values as compared to GDL concentrations. Figure 1B shows the average final pH values with errors associated with different gelator concentrations explored in this study (2–20 mM) for each given concentration of GDL.

[a] *V. Lakshminarayanan, C. Chockalingam, Dr. E. Mendes, Dr. Prof. J. H. van Esch*
Advanced Soft Matter, Department of Chemical Engineering
Delft University of Technology
Van der Maasweg 9, 2629HZ, Delft, The Netherlands
E-mail: j.h.vanesch@tudelft.nl

Supporting information for this article is available on the WWW under https://doi.org/10.1002/cphc.202100276

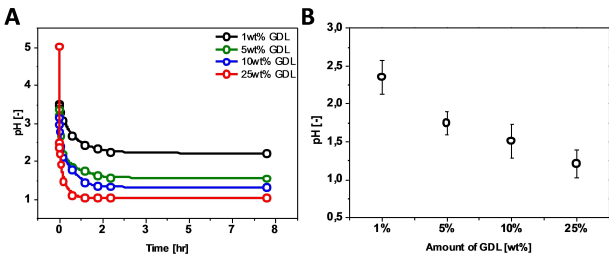

Figure 1. A) GDL dependence of pH change for the case of 5 mM Na_2DBC. B) Final pH values measured after 8 hours from addition of 1 wt.% (57 mM), 5 wt.% (295 mM), 10 wt.% (624 mM) and 25 wt.% (1871 mM) of GDL. The corresponding [GDL]/[Gelator] molar ratios are 11, 59, 125 and 374 respectively, Error bars indicate final pH variation (standard deviation, N = 3) at 5 mM gelator concentration.

The data for 2, 10 and 20 mM Na_2DBC can be found in Figures S1–S3 of the supplementary information. The variation in end pH values with DBC and GDL concentration is presented in Table S1. The variation in the pH values with gelator concentration can be qualitatively explained by considering the buffer formation by the protonation of DBC salt (Na_2DBC). With increase in initial DBC salt concentration, the buffer capacity increases slightly for a given amount of GDL. However, for a fixed amount of DBC salt, increasing the GDL concentration enables the system to overcome the buffer capacity of the DBC buffer resulting in the lowering of the end pH. We want to highlight to the reader that while GDL is a useful tool to control kinetics, it could be challenging in deploying it as a quantitative indicator. To understand if [GDL]/[DBC salt] could be used a quantitative indicator we plotted the end pH at various molar ratios (see Figure S26 in the Supporting Information). The results showed scattering of values leaving us to omit the use of molar ratios as a way of representing the data. We hence continued to use the absolute concentrations to represent data in this work. We next investigated the gelation of DBC in the presence of GDL. It has been reported for DBC that gelation occurs when pH drops below the pKa.[16,17] The gelation occurs via formation of fibres through self-assembly of the gelators. Since the gel formation in our system is coupled to the kinetics of the pH change, a technique that can track a material property that varies as a function of time is required. The dynamic storage and loss moduli (G′ & G″) are material properties that are commonly reported for supramolecular gels and rheological techniques are commonly reported to track kinetics of gel formation.[15] Hence, we followed the kinetics of gelation of GDL triggered DBC gels under the rheometer. The results obtained for 5 mM of gelator is given in Figure 2. The data for 2, 10 and 20 mM gelator can found in Figures S4–S6. As it can be observed in Figure 2 for low GDL concentrations, the observed G′ does not start increasing immediately after the addition of GDL. There is a time delay of (lag phase) after which gelation begins and reaches a plateau after sometime (ca. 30 min). This is similar to earlier reported work on gelation of LMWG with GDL in the case of Fmoc-dipeptide gelators.[18] The hydrolysis of GDL produces acid that protonates the carboxylate ions of DBC. The protonated DBC (H_2DBC) then proceeds to form a gel via self-assembly. The hydrogen bonding between carboxylic acid groups in the gelator has been found to be crucial in the fiber network formation in this class of gelators.[19] With increasing amounts of added GDL, the lag phase reduces in time, indicating that self-assembly of gelator molecules happens earlier. At very high concentrations of GDL, pH drops below the pKa (3.58) within the first 30 seconds, enough to initiate the formation of fibres.[17] Gelation is said to have occurred when a fibrous network consisting of entanglements or crosslinks has been formed that begins to offer resistance to the applied shear. Experimentally, this is defined as the point when G′ = G″. Recent works on LMWGs have suggested that this definition is only approximate and not binding.[18] For gelation of non-crystalline solids, an accurate method for predicting t_{gel} has been suggested by plotting (s/tanδ) vs. time (s – standard deviation in tanδ, tanδ = G″/G′) and choosing the value of minimum of this curve.[20] In our efforts to use this method on our data, we observed that the t_{gel} values determined by this method were much larger than experimentally observed. We hence continued with our first choice, and we take the time for gelation (t_{gel}), as the point where G′ crosses G″. The time-sweep curves for the remaining gel concentrations and tanδ plots can be found in the supplementary section (see Figures S21–S24). For a given concentration of gelator, increasing the amount of GDL leads to a decrease in the observed gel point (see Figure 3). The same trend is observed for the plateau modulus. Faster hydrolysis seems to result in weaker gels, an observation that also has been reported for GDL triggered Fmoc-dipeptide hydrogels.[21] However, the role of kinetics was not considered to as important as compared to end pH in the case of Fmoc-dipeptide hydrogels.[30] From our observations, there seems to be an optimum (around 5–10% GDL) depending on the gelator concentation where G′ achieves a maximum before decreasing further. This is likely linked to a change in the type of network being formed in the gel. In our efforts to investigate this, we took inspiration from earlier reported work on temperature-triggered organogelators whose structure-property relationships have been studied in detail over many years.[10,22,23]

Temperature triggered formation of fibrous organogels from N-layroyl-L-glutamic acid di-n-butylamide (GP-1) has been investigated by X.Y. Liu and co-workers to develop rheology-based models and analysis in terms of the fractal dimensions of their networks.[22] Their model was based on the Avrami model to describe nucleation and growth of bulk crystals [Eq. (1)]:

$$\ln[1 - X_{cr}] = -k\left(t - t_{gel}\right)^{D_{f,A}} \quad (1)$$

In Equation (1), k is constant, X_{cr} is the crystallinity of the system which is equal to the ratio of volume fraction of crystal material at time t to the volume fraction as $t \to \infty$, and t_{gel} is the time for gelation or gel point as determined by rheology. The authors correlated crystallinity and viscosity by using Einstein's relation to end up with the following relation:[23,24]

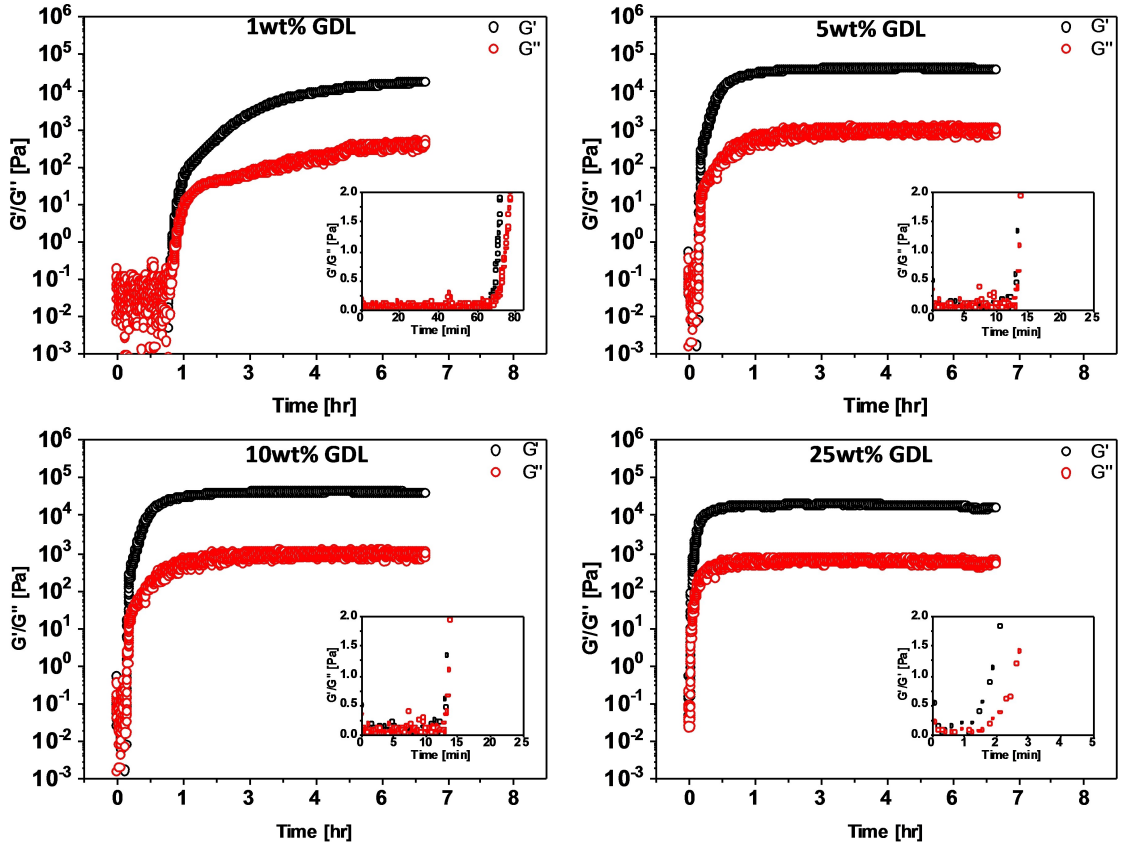

Figure 2. Time evolution of storage modulus (G′) and loss modulus (G″) upon addition of different amounts of GDL to 5 mM Na_2DBC solution (1 wt.% (57 mM), 5 wt.% (295 mM), 10 wt.% (624 mM) and 25 wt.% (1871 mM) of GDL. The corresponding [GDL]/[Gelator] molar ratios are 11, 59, 125 and 374 respectively). The insets show the early stages of gelation that are used in determining the gel point.

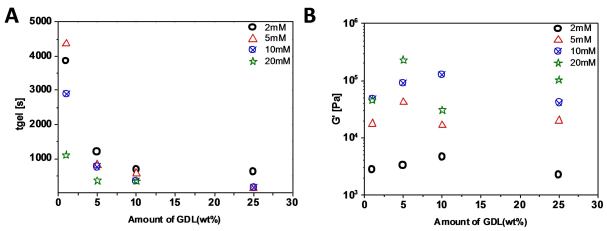

Figure 3. Plots of t_{gel} (A) and plateau modulus $[G'(\infty)]$ (B) as a function of concentration of GDL (1 wt.% (57 mM), 5 wt.% (295 mM), 10 wt.% (624 mM) and 25 wt.% (1871 mM) of GDL) at various gelator concentrations. Expanded version for Figure 3B available in the Supporting Information as Figure S25.

$$X_{cr}(t) = \frac{\varphi(t)}{\varphi(\infty)} = \frac{\eta_{sp}(t)}{\eta_{sp}(\infty)} = \frac{\eta^*(t) - \eta_0}{\eta^*(\infty) - \eta_0} \quad (2)$$

In Equation (2), $\varphi(t)$ and $\varphi(\infty)$ are the volume fractions at time t and $t \to \infty$ respectively, and $\eta_{sp}(t)$ and $\eta_{sp}(\infty)$ are the corresponding specific viscosities. The complex viscosities $\eta^*(t)$ and η_0 of the system and the solvent, respectively, are related to the complex moduli, G^* of the system to give the following final relation:

$$X_{cr}(t) = \frac{\varphi(t)}{\varphi(\infty)} = \frac{\eta_{sp}(t)}{\eta_{sp}(\infty)} = \frac{\eta^*(t) - \eta_0}{\eta^*(\infty) - \eta_0} = \frac{G^*(t) - G^*_0}{G^*(\infty) - G^*_0} \quad (3)$$

By using Equation (3), the time dependent values of $X_{cr}(t)$ can be obtained from the time evolution of the complex moduli $G^*(t)$, which can now be analysed with Equation (1) by plotting $\ln\{-\ln[1 - X_{cr}(t)]\}$ vs. $\ln[t - t_{gel}]$ to yield the fractal dimension D_f. For one-dimensional or rod-like growth, two-dimensional or plate-like growth, and 3-dimensional spherical growth, $D_f = 1,\ 2,\ 3$ respectively. The value of D_f indicates the fractal dimension, an indication of self-similarity in the network. By comparing with results from static light scattering data, it has been shown that their method gave very good estimates for the dimensionality of their system.[3,25] In later accounts, another method based on the Dickinson model developed by Terech and co-workers was used instead of the above Avrami relation.[26,27] The reason cited was that the Avrami exponent depends strongly on both crystal growth dimensionality and nucleation mechanism. Furthermore, they introduced a scaling argument into the Dickinson model to create an Extended-Dickinson Model that provided good estimates for dimensionality of the structures when compared against optical microscopy images. The same model was later used to study the

effect on confinement on molecular gelation of GP-1 at higher concentrations (3-7 wt.%).[27] In our work, the maximum concentration of gelator was 20 mM (ca. 1 wt.%). Hence the original Dickinson model which is valid for semi-dilute systems maybe be used to check if it might be applicable. In this model, instead of crystal volume fraction, a gel-volume fraction as defined in previous work is used.[26,27] This volume fraction is directly related to the storage modulus instead of the complex modulus. The final expression is given by Equation (S1) in the Supporting Information.

Therefore, a plot of gel volume fraction vs. the time during the growth phase can be used to extract the exponent from which the fractal dimension can be calculated. From the analysis of rheology data based on the models, we observed that the obtained values are strongly dependent on the region chosen for the fitting process. The regions just after $t > t_{gel}$ have been chosen in the previously reported work..[22,23,27] Since the plots need $t - t_{gel}$ (see Figure 4) the estimates depend on the value of t_{gel}. As mentioned in the methods section, a time delay between vortexing and eventually starting the measurement was observed. This means that the true gelation time is somewhere in the vicinity of the chosen gelation time, that is, early growth stages. We observed that the exponent values obtained from both models do not differ significantly (see Figures 4, S7, S8, S9, S10). However, this leads to different fractal dimensions because the two models have different relationships between exponent and fractal dimension. In the Avrami model exponent 'n' of Figure 4 is directly equal to the fractal dimension $D_{f,A}$ and we see that it increases as the concentration of GDL increases. In the case of the Dickinson model, we observe the opposite trend with $D_{f,D}$ decreasing as the GDL amount is increased (see Figures 5, S11, S12, S13, S14 and Table S3) as also shown from equation S1. This discrepancy arises from the reciprocal relationship which exists in the Dickinson model. We hence used the Avrami model predictions for further investigation. To reconcile the model predictions visually, we performed confocal microscopy (CLSM) experiments as described in the experimental section and the results are shown in Figure 5. The CLSM micrographs exhibit differences in the morphology of hydrogels (Figure 5, B–E) based on the concentration of GDL. At lower concentrations of GDL, entangled fibrous networks are observed which becomes more inhomogeneously distributed at higher concentrations. Similar observations were made with Fmoc-dipeptide hydrogels that were produced by acidification using HCl.[14] A sharp decrease in pH is associated with this microstructure feature. In our system, higher concentrations of GDL cause a rapid reduction of pH which can lead to such microstructural inhomogeneities. Previous work on non-peptide low molecular weight gelators has shown that sharp decrease in pH lead to fibrillar gels with side-branches and spherulites.[28]

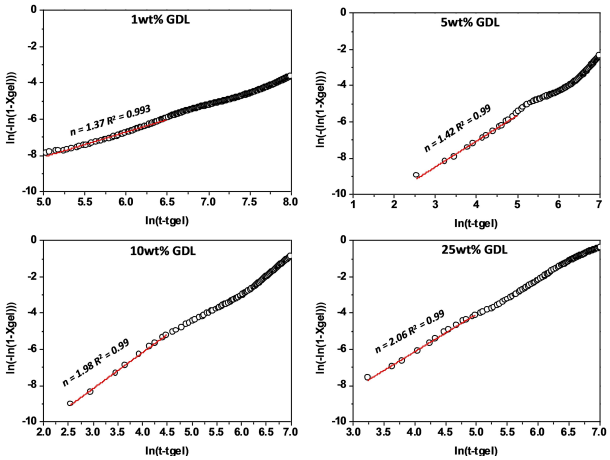

Figure 4. Model fits based on Avrami model for the case of 5 mM gelator concentration and different amounts of GDL (1 wt.% (57 mM), 5 wt.% (295 mM), 10 wt.% (624 mM) and 25 wt.% (1871 mM) of GDL). The corresponding [GDL]/[Gelator] molar ratios are 11, 59, 125 and 374 respectively.

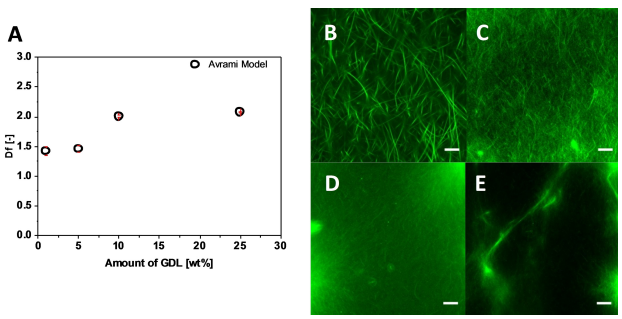

Figure 5. Model predictions for $D_{f,A}$ (A). False-colour CLSM micrographs showing differences in morphology in hydrogels formed from 5 mM of gelator upon addition of 1 wt.% (57 mM) (B), 5 wt.% (295 mM) (C), 10 wt.% (624 mM) (D) and 25 wt.% (1871 mM) € of GDL. The corresponding [GDL]/[Gelator] molar ratios are 11, 59, 125 and 374 respectively. Scale bar is 20 μm.

From the model predictions we see in an increase in $D_{f,A}$ as the concentration of GDL increases. Figure 5A illustrates this for the case of 5 mM of DBC gelator. Similar observations are seen for the case of 2 mM, 10 mM and 20 mM gelators as the concentration of GDL trigger increases (Figures S12A, S13A and S14A in ESI). From work on pH-triggered self-assembly of sophorolipids, we can see that at high acidification rates, the tendency to side-branch and form spherulites increases leading to weaker gels that are loosely connected. DBC is also known to form spherulites in water when gels produced by cooling down a hot solution were allowed to stand over a long period of time.[29] From confocal micrographs we do see observe the presence of loosely connected spherulites at higher concentrations of GDL (Figures 5D, 5E, S12D, S12E, S13D, S13E, S14C). Correspondingly we do observe an increase in Df from ca. 1.2 (at 1% GDL) to 1.5–3 (at 25% GDL) (see Table S2 in ESI). From CLSM data, it can be seen that a faster decrease in pH produces more in-homogenous loosely connected structures as opposed to thinner fibres at around 5% GDL. It is known that thinner, homogenously distributed fibres provide more strength to the network.[29] This could explain the apparent increase in storage modulus seen during the rheological characterization. At lower concentrations of GDL, Avrami model predictions indicate that a nearly one dimensional (1D) fibrous structure exists which

corroborates well with the CLSM micrographs. With increasing gelator concentration, the Avrami model predicted fractal dimension increases as the driving force (acidification rate) increases. Avrami model considers the network formation to be similar to the process of crystallization which is applicable to DBC since they are known to form crystals in aqueous environments.[31] The Dickinson model developed for weak interacting colloidal aggregation does not provide estimates of fractal dimension that corroborate well with experimental observations made using confocal microscopy. The model assumes that particles and aggregates can be treated as spheres.[32] The aggregates behaving like hard spheres form space-filling structures in a diffusion or reaction limited aggregation mechanisms. The fractal dimension relates to the gelation time with near-infinite gelation times for compact structures ($\mathbf{D_f} = 3$). In our systems gelation time is dependent on gelator concentration and trigger concentration. Furthermore, Dickison model does not take any side-branching or interpenetration into account. For these reasons, it is not considered an appropriate model to understand structure-property relationships in pH-triggered LMWG systems despite its moderate success in organogelator systems. The Avrami model predicted fractal dimensions are consistent with previously reported values for organogelators and chemical triggered systems.[15,22,23] However the transition between nearly 1-D fibers at low trigger concentrations (1% GDL) to loosely connected spherulites at higher trigger concentration (10%, 25% GDL) seems to indicate that there is a regime where tendency to side-branch begins to increase. We wonder if there may be a threshold concentration of gelator and trigger which could exist in these systems. However, based on the experimentally studied concentrations, we are unable to draw definitive conclusions at this stage.

3. Conclusions

This work shows that mechanical properties of low molecular weight gelators are dependent on kinetics of GDL hydrolysis, an observation that differs from previous work on Fmoc-di peptide gelators and more in line with sophorolipids.[28,30] Rheology analysis using Avrami based kinetic-fibre branching models developed for organogelators give a good indication of fractal dimensions for pH-triggered LMWGs such as DBC when acidified using a trigger such as GDL. Through careful experimental design with smaller steps in trigger and gelator concentration, it would be possible to explore the transition between 1-D fibers to networks with side-branches and spherulites. This would enable us to precisely control the morphology of gel networks which could be valuable for applications in cell culturing, tissue engineering where morphology of scaffolds can have an impact on cell proliferation and differentiation.[1]

Experimental Section

Materials and Methods

Safety and Hazards

This work was carried out in a Chemistry lab with personal protective equipment such as lab coat and safety eyewear. Powdered solid materials were handled with care to avoid accidental inhalation and nasal irritation. Exercise caution while handling chemicals and handle them as per the safety protocols of your laboratory.

Gelator and pH Triggering Agents

N–N'Dibenzoyl-L-cystine (98%), nile red (9-diethylamino-5-benzo[α] phenoxazion), and Sodium Hydroxide were purchased from Sigma-Aldrich and used without further purification. Glucono-δ-lactone (99%) was purchased from Alfa Aesar and used without further purification.

Production of Hydrogels

Neutralized DBC salt (Na_2DBC) stock solutions were first prepared fresh by preparing a solution from a weighted amount of the free acid gelator (H_2DBC) and the corresponding volume of a 1 M NaOH stock solution containing two equivalents of base. The mixture was vortexed to ensure complete dissolution of the gelator. The pH was then measured to and found to be around 4–5. Variance across batches was tested and found to be small (4.81 ± 0.68). To prepare the hydrogels, measured quantities of GDL (in the form of a powder) were added to Na_2DBC solutions and vortexed briefly and allowed to set. The dissolution of GDL is faster than its hydrolysis and this results in a gradual decrease in pH which eventually leads to gel formation.[14]

pH Measurements

All pH measurements were carried out using a Metrohm 744 pH meter at 25 °C after calibrating using standard pH buffers at pH 1.61, 4 and 7.

Rheological Characterisation

Oscillatory rheology measurements were performed on an AR-G2 strain-controlled rheometer (TA instruments) using a 40 mm stainless steel plate-plate geometry. The temperature was maintained at 25 ± 0.2 °C. A known amount of GDL was put in a 2 mL vial with an easy open cap. Measured quantity of DBC salt solution was aspirated in a 1000 μL micropipette and added to the vial. After a quick vortexing, the solution was casted on to the bottom plate of the rheometer. A short time delay of 6 seconds was observed between vortexing, to casting and lowering of the top plate to the bottom plate. A solvent trap filled with water or hexadecane was used to prevent drying of the formed hydrogels. Time evolution of storage (G') and loss modulus (G'') was followed at 1 Hz and 0.05% strain. This is a commonly used setting for measuring gels formed from LMWGs.[15] To be thorough, the LVER (Linear Viscoelastic region) was confirmed at these settings via frequency and strain sweeps (Figures S15–S18 in ESI). To allow comparison across different samples, a constant gap of about 770 ± 10 μm was maintained. Rheology measurements which were used to estimate fractal dimension were carried out in triplicate.

Confocal Laser Scanning Microscopy (CLSM)

Morphology visualization of hydrogels were performed using a Zeiss LSM 710 confocal laser scanning microscope. Nile red was used as the staining agent to be able to monitor and track the DBC gel fibres.[16] The hydrogel samples were prepared by mixing 40 μL of 5 mM Nile Red in 95% pure ethanol to a weighed amount of GDL along with a predetermined volume of Na_2DBC solution and MilliQ water as required for a certain hydrogel concentration in a 1 ml vial. The final concentration of Nile red in this solution was 25 μM. The solution was then vortexed for 30 seconds to ensure complete dissolution of GDL. 80 μL of this solution was pipetted out and placed in a chamber made of glass slide (2×2 cm) and an inert rubber gasket which was again sealed with a second glass side. The slides were mounted on the stage of the microscope. CLSM micrographs of the hydrogels were obtained using a laser beam at 514 nm and oil immersion 40× Zeiss objective.

Acknowledgements

The authors thank Ben Norder and Matija Lovrak for their help with rheology and CLSM measurements respectively. The authors also would like to thank NanoNextNL for funding this research under programme 07A.11.

Conflict of Interest

The authors declare no conflict of interest.

Keywords: hydrogelator · rheology · kinetics · fractal dimension · confocal microscopy

[1] V. Le Sage, V. Lakshminarayanan, E. Mendes, R. Eelkema, J. Van Esch, *Chim. Oggi-Chem. Today* **2014**, *32*.
[2] A. Friggeri, B. L. Feringa, J. van Esch, *J. Controlled Release* **2004**, *97*, 241–248.
[3] E. R. Draper, L. L. E. Mears, A. M. Castilla, S. M. King, T. O. McDonald, R. Akhtar, D. J. Adams, *RSC Adv.* **2015**, 95369–95378.
[4] E. R. Draper, E. G. B. Eden, T. O. McDonald, D. J. Adams, *Nat. Chem.* **2015**, *7*, 848–852.
[5] G. Cravotto, P. Cintas, *Chem. Soc. Rev.* **2009**, *38*, 2684.
[6] J. Boekhoven, A. M. Brizard, K. N. K. Kowlgi, G. J. M. Koper, R. Eelkema, J. H. van Esch, *Angew. Chem.* **2010**, *122*, 4935–4938; *Angew. Chem. Int. Ed.* **2010**, *49*, 4825–4828.
[7] D. J. Cornwell, D. K. Smith, *Mater. Horiz.* **2015**, *2*, 279–293.
[8] J.-L. Li, R.-Y. Wang, X.-Y. Liu, H.-H. Pan, *J. Phys. Chem. B* **2009**, *113*, 5011–5015.
[9] J. L. Li, X. Y. Liu, *Adv. Funct. Mater.* **2010**, *20*, 3196–3216.
[10] J. L. Li, X. Y. Liu, C. S. Strom, J. Y. Xiong, *Adv. Mater.* **2006**, *18*, 2574–2578.
[11] E. R. Draper, L. L. E. Mears, A. M. Castilla, S. M. King, T. O. McDonald, R. Akhtar, D. J. Adams, *RSC Adv.* **2015**, *5*, 95369–95378.
[12] D. J. Adams, M. F. Butler, W. J. Frith, M. Kirkland, L. Mullen, P. Sanderson, *Soft Matter* **2009**, *5*, 1856.
[13] F. M. Menger, K. L. Caran, *J. Am. Chem. Soc.* **2000**, *122*, 11679–11691.
[14] D. J. Adams, M. F. Butler, W. J. Frith, M. Kirkland, L. Mullen, P. Sanderson, *Soft Matter* **2009**, *5*, 1856.
[15] J. Boekhoven, J. M. Poolman, C. Maity, F. Li, L. van der Mee, C. B. Minkenberg, E. Mendes, J. H. van Esch, R. Eelkema, *Nat. Chem.* **2013**, *5*, 433–7.
[16] J. Boekhoven, W. E. Hendriksen, G. J. M. Koper, R. Eelkema, J. H. van Esch, *Science* **2015**, *349*.
[17] J. P. Wojciechowski, A. D. Martin, P. Thordarson, *J. Am. Chem. Soc.* **2018**, *140*, 2869–2874.
[18] A. Z. Cardoso, A. E. Alvarez Alvarez, B. N. Cattoz, P. C. Griffiths, S. M. King, W. J. Frith, D. J. Adams, *Faraday Discuss.* **2013**, *166*, 101.
[19] F. M. Menger, Y. Yamasaki, K. K. Catlin, T. Nishimi, *Angew. Chem. Int. Ed. Engl.* **1995**, *34*, 585–586.
[20] E. Rudé Payró, J. Llorens Llacuna, *J. Non-Cryst. Solids* **2006**, *352*, 2220–2225.
[21] A. Z. Cardoso, A. E. Alvarez Alvarez, B. N. Cattoz, P. C. Griffiths, S. M. King, W. J. Frith, D. J. Adams, *Faraday Discuss.* **2013**, *166*, 101.
[22] X. Y. Liu, P. D. Sawant, *Appl. Phys. Lett.* **2001**, *79*, 3518–3520.
[23] X. Y. Liu, K. Maiwa, K. Tsukamoto, *J. Chem. Phys.* **1997**, *106*, 1870–1879.
[24] A. Einstein, *Ann. Phys.* **1906**, *324*, 371–381.
[25] D. J. Adams, M. F. Butler, W. J. Frith, M. Kirkland, L. Mullen, P. Sanderson, *Soft Matter* **2009**, *5*, 1856.
[26] R.-Y. Wang, P. Wang, J.-L. Li, B. Yuan, Y. Liu, L. Li, X.-Y. Liu, *Phys. Chem. Chem. Phys.* **2013**, *15*, 3313–9.
[27] Y. Liu, W.-J. Zhao, J.-L. Li, R.-Y. Wang, *Phys. Chem. Chem. Phys.* **2015**, *17*, 8258–65.
[28] C. G. Wolf, E. K. Rideal, *Biochem. J.* **1922**, *16*, 548–555.
[29] G. Ben Messaoud, P. Le Griel, D. Hermida-Merino, S. L. K. W. Roelants, W. Soetaert, C. V. Stevens, N. Baccile, *Chem. Mater.* **2019**, *31*, 4817–4830.
[30] A. Z. Cardoso, A. E. Alvarez Alvarez, B. N. Cattoz, P. C. Griffiths, S. M. King, W. J. Frith, D. J. Adams, *Faraday Discuss.* **2013**, *166*, 101–116.
[31] F. M. Menger, Y. Yamasaki, K. K. Catlin, T. Nishimi, *Angew. Chem. Int. Ed. Engl.* **1995**, *34*, 585–586.
[32] E. Dickinson, *J. Chem. Soc. Faraday Trans.* **1997**, *93*, 111–114.

Manuscript received: April 10, 2021
Revised manuscript received: July 16, 2021
Accepted manuscript online: July 20, 2021
Version of record online: October 7, 2021